Research Article

Vu Viet Quyen* and Nguyen Duong Nam

Research on the magnesium reduction process by integrated calcination in vacuum

https://doi.org/10.1515/htmp-2025-0074
received September 02, 2024; accepted February 11, 2025

Abstract: At present, the predominant method for magnesium production relies on the Pidgeon process, a straightforward yet inefficient procedure characterized by high energy consumption and substantial greenhouse gas emissions. In order to foster advancements in magnesium production technology, this study explored an approach that consolidates silicon calcination and thermal reduction stages into a single stage. The main raw material used in this process is dolomite powder, which replaces the previously calcined dolomite. The primary objective of this novel approach is to streamline production timelines, enhance coherence between stages, and curtail energy usage in magnesium production. The investigation delves into the impact of dolomite decomposition temperature and forming pressure on the efficiency of the integrated process. Laboratory-scale experimentation revealed that the optimal decomposition temperature is 800°C. While the forming pressure significantly influenced the reduction rate, it did not markedly impact the final reduction efficiency. A forming pressure of 150 MPa yielded the highest reduction rate. This decrease is attributed to the dissociation of reactants during dolomite decomposition, indicating a need for further research to address the reduction in contact area during the degradation stage and enhance the efficiency of this integrated process.

Keywords: magnesium production, integrated process, dolomite powder, decomposition temperature

1 Introduction

Production of Mg using the silicon heat method, typically the Pidgeon process, is extensively employed for magnesium production across numerous countries worldwide. This method is celebrated for its simplicity, eschewing the need for modern equipment or intricate techniques, and its adaptability allows for easy adjustments to meet production demands, particularly suitable for the conditions prevalent in developing countries [1,2]. However, inherent drawbacks include batch production, resulting in intermittent operation and subsequently lower productivity, substantial requirements for handling waste residue's environmental impact post-production, labor-intensive operations, and notably high energy consumption compared to alternative reduction methods [3,4]. Given the endothermic nature of the dolomite reduction reaction (ΔH = ~209 kJ·mol^{-1} Mg), the Pidgeon process demands a significant level of heat input, necessitating substantial energy provision for industrial reactors. Statistical analysis conducted by Ramakrishnan and Koltun regarding the various stages of Mg production using the Pidgeon process, from dolomite ore mining to Mg ingot production, revealed significant energy consumption throughout the process [5]. Notably, the dolomite ore calcination and reduction phase in the vacuum furnace emerged as the most energy-intensive, accounting for approximately 70% of the total energy consumption. It is reported that Mg production through the Pidgeon process consumes 1.6 times more energy and emits greenhouse gases compared to aluminum production and 1.5 times that of Mg production using the thermocarbon method [6,7].

The Pidgeon method operates in batches, differing from continuous processes like Mintek or Magnetherm [8]. The dolomite calcination stage occurs in a separate furnace. Upon completion, the furnace requires cooling to remove the calcined dolomite, resulting in significant heat release into the surroundings, leading to energy wastage. Following grinding, mixing, and briquetting, the mixture undergoes a reduction in a vacuum tube, necessitating a substantial increase in furnace temperature from

---

* **Corresponding author: Vu Viet Quyen**, The School of Mechanical Engineering, Vietnam Maritime University, Haiphong, 180000, Vietnam, e-mail: quyenvv.cndt@vimaru.edu.vn
Nguyen Duong Nam: The School of Mechanical Engineering, Vietnam Maritime University, Haiphong, 180000, Vietnam

ambient levels [9]. This phase also consumes significant heat energy, while some heat generated during dolomite firing not being recycled. This inefficiency arises from the process interruption between the calcination and reduction stages. Continuous integration of these stages would enable the heat generated during dolomite heating to be seamlessly utilized for the subsequent reduction stage, minimizing heat loss to the environment. Additionally, this process exhibits prolonged cycle times for individual stages. Conversely, combining the calcination and reduction stages would streamline the process, reducing cycle duration and enhancing productivity by enabling more cycles within the same timeframe. To further enhance the traditional Pidgeon process, improved pelleting methods integrated with calcination and silicothermic reduction have been developed [10–12]. In the integration process, dolomite powder, derived from dolomite ore, is mixed with ferrosilicon and CaF_2 to form pellets. The entire calcination and thermal reduction occur within a retort. The heat generated from dolomite decomposition will be partially reused for silicothermic reduction, and the CO_2 released during this process can be efficiently collected and recycled through a vacuum system. Numerous studies have demonstrated that altering the conditions for dolomite decomposition results in mixtures with varying properties, which can influence the subsequent reduction stage [13]. Additionally, increasing the hydration activity of calcined dolomite has a significant effect on the reduction cycle time and enhances the magnesium extraction yield [14]. The calcination of dolomite is conducted at elevated temperatures, which results in significant material loss due to thermal decomposition. Furthermore, the ferrosilicon reducing agent, when pre-mixed within the calcination mixture, is susceptible to oxidation in the CO_2-rich atmosphere generated during the decomposition of dolomite. The calcination of dolomite in two stages – a low-temperature stage for decomposing $MgCO_3$ followed by a high-temperature stage for decomposing $CaCO_3$ – demonstrated a significant reduction in dolomite loss due to combustion [15]. This evidence suggests that operating the calcination process at reduced temperatures may mitigate both the oxidation of the ferrosilicon reductant and the loss of dolomite. Such an approach can be realized by performing calcination in a vacuum environment, which, as indicated by thermodynamic analyses, establishes conditions that lower the decomposition temperature of dolomite. Consequently, the proposed methodology entails the calcination of pre-prepared pellets under vacuum conditions in a two-stage process.

In this study, Vietnamese dolomite powder was used in an integrated process to evaluate the impact of the calcination stage on magnesium reduction efficiency. During the calcination stage, the pellets were calcined in a vacuum environment with a low-temperature calcination stage to decompose $MgCO_3$ and a high-temperature calcination stage to decompose $CaCO_3$.

2 Materials and methods

2.1 Thermodynamics

When dolomite is calcined, the decomposition process proceeds as follows:

$$MgCO_{3(s)} - MgO_{(s)} + CO_{2(g)}, \tag{1}$$

$$CaCO_{3(s)} - CaO_{(s)} + CO_{2(g)}. \tag{2}$$

The database, implemented in FactSage 7.2 software, was utilized to calculate the ΔG–T relationship for each decomposition reaction under a vacuum of 1,000 Pa. As shown in Figure 1, the Gibbs free energy of reactions (1) and (2) decreased significantly with increasing temperature in the vacuum environment. $MgCO_3$ began to decompose at approximately 300°C, while $CaCO_3$ decomposition occurred around 600°C. These temperatures were considerably lower than the standard calcination temperatures for dolomite, typically ranging from 900°C to 1,100°C. With increasing temperatures, the decomposition reaction rates increased; therefore, the calcination temperature for $MgCO_3$ decomposition was set at 500°C, and for $CaCO_3$

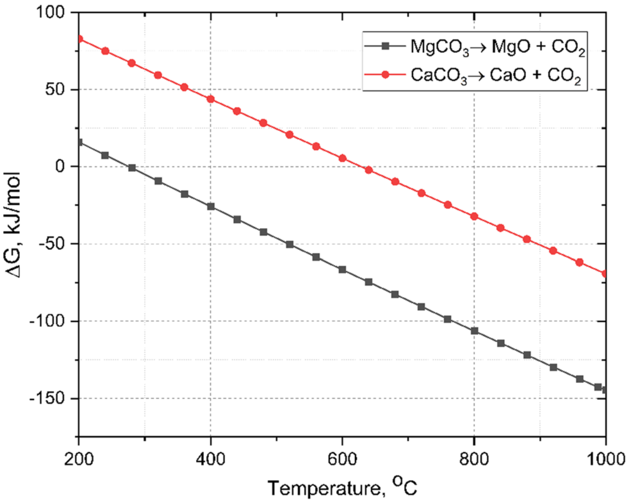

Figure 1: Relationship between the Gibbs free energy of the decomposition reactions and temperature under vacuum conditions of 1,000 Pa.

decomposition, the temperature range of 700°C–1,000°C was selected for evaluation.

2.2 Raw materials and experimental procedure

This study used dolomite ore and ferrosilicon alloy (75%) produced in Vietnam and CaF_2 (98%) produced in China as raw materials. The chemical composition of dolomite ore and ferrosilicon alloy is shown in Table 1.

The dolomite ore was pulverized into a fine powder and combined with ferrosilicon and fluorite alloy in a ratio of 86.7:11.5:1.8, corresponding to a 20% silicon ratio as per the Pidgeon process. Subsequently, the mixture underwent milling in a planetary ball mill model NQM-4 of Yangzhou Nuoya Machinery until reaching a particle size of 100 mesh. Following milling, the mixture was briquetted into pellets under different pressures of 60, 80, 100, 120, and 150 MPa, with each pellet weighing approximately 20 g.

Table 1: Chemical elements of dolomite ore and ferrosilicon alloy

Dolomite ore						
MgO	**CaO**	**SiO_2**	**Fe_2O_3**	**Al_2O_3**	**Others**	**Loss of ignition**
20.25	30.8	0.36	0.53	0.12	0.21	47.73
Ferrosilicon alloy						
Si	**Fe**	**C**	**P**	**S**	**Mn**	**Al**
74.4	24.1	0.1	0.04	0.01	0.35	1.0

The experimental procedure was carried out according to the flow diagram in Figure 2. In the first step, the sample consisting of five pellets is placed in an alumina boat, which is then placed in the retort and securely covered. The second stage is the calcination process, in which the furnace is raised to the first calcination temperature of 500°C for 0.5 h. To study the effect of the decomposition temperature during the calcination stage on the reduction efficiency, the second calcination temperature is gradually increased to 700, 800, 900, and 1,000°C for an additional 0.5 h. Throughout this process, the vacuum pump and pressure regulator are activated to maintain a pressure of 1,000 Pa, facilitating the removal of CO_2 gas generated within the retort via the vacuum pipeline system. After calcination, the temperature was gradually transitioned to the reduction stage. To accurately measure the reduction rate, argon gas was introduced into the furnace to restore atmospheric pressure, and the vacuum pump system was halted. This step prevents unwanted reduction reactions during the thermal transition. The retort was then heated from the calcination temperature to 1,250°C for the reduction stage. Upon reaching 1,250°C, the cooling water system and vacuum pump were activated to lower the pressure in the retort to 100 Pa. Subsequent to the conclusion of the reduction process,

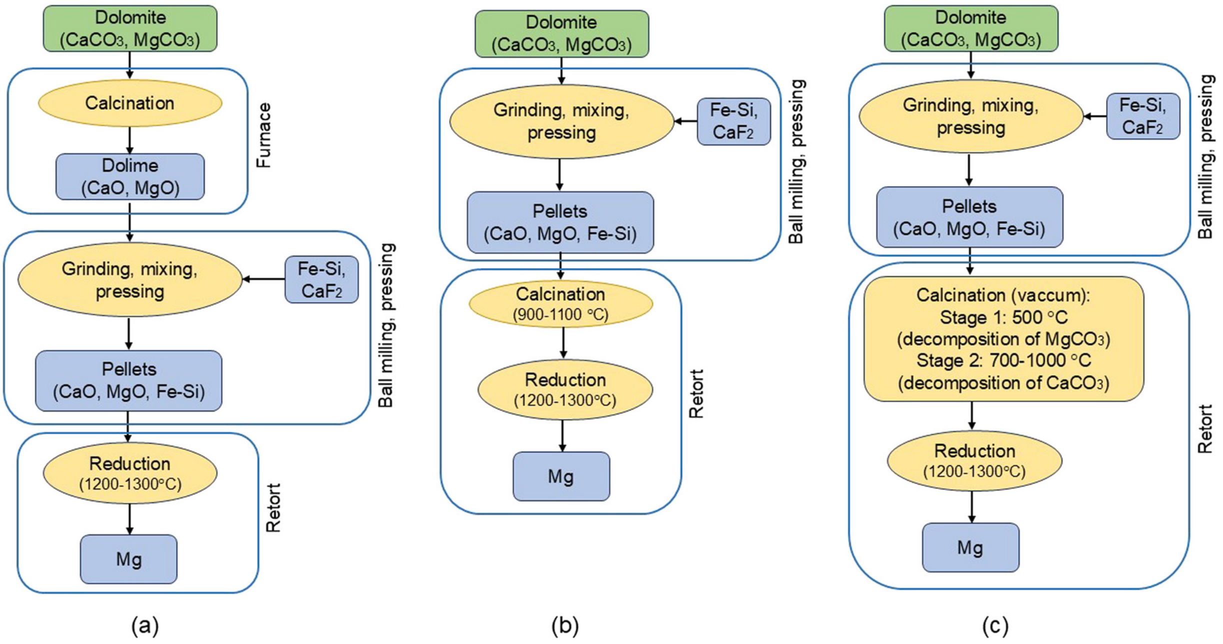

Figure 2: Process comparison of (a) Pidgeon, (b) integrated process, and (c) integrated vacuum calcination process of this study.

the products within the crystallization zone and any remaining residue are collected and subjected to analysis.

The reduction efficiency in the integrated process is determined using the following formula:

$$\text{reduction efficiency (\%)} = \frac{w_2}{w_1}\cdot 100,$$

where w_1 is the mass of Mg in the initial mixture and w_2 is the mass of metallic Mg obtained in the cooling zone.

The experimental apparatus used is shown in Figure 3. The apparatus consists of a vacuum pump ULVAC PX-202 using an SM-ZSE30 gauge and an argon gas cylinder connected to a retort. The retort, constructed from 310S stainless steel, is heated by a furnace using a SiC heating rod controlled by a platinum/rhodium thermocouple. The retort head, where magnesium crystallizes, is equipped with a water-cooling system.

3 Results and discussion

3.1 Magnesium products

The reconstituted product derived from the combined process is depicted in Figure 4, showcasing granular magnesium crystals reminiscent of those obtained through the Pidgeon process. In the initial region of the crystallization zone adjacent to the reduction area, sizable magnesium crystals ranging from 0.5 to 2 mm are observed. The scanning electron microscopy (SEM) image of metallic magnesium in Figure 4(b) reveals the presence of impurities on the surface of the magnesium particles.

The results of energy-dispersive X-ray spectroscopy (EDS) analysis indicate that these surface impurities primarily consist of magnesium, oxygen, and trace amounts of carbon. Upon comprehensive analysis, it is evident that the product obtained from this integrated process closely resembles that of the Pidgeon process. Analysis of Mg content in product samples reached 98.56%.

3.2 Effect of decomposition temperature on reduction efficiency

In the Pidgeon process, the calcination stage operates independently of the reduction stage. However, in the combined process, these stages occur consecutively within the same retort; thus, the calcination temperature is anticipated to exert a significant influence on reduction efficiency.

The pellets used to determine the effect of decomposition temperature were briquetted at a pressure of 60 MPa. The time taken in the reduction phase is 3 h. The highest reduction efficiency recorded during the experiment examining the influence of calcination temperature was 73.5%, which was achieved with a first-step calcination temperature of 500°C followed by a second-step temperature of 800°C over a total duration of 1 h. This efficiency is 4.1% lower than that of the Pidgeon process under equivalent reduction temperature conditions of 1,250°C [3]. Figure 5 illustrates a slight increase in magnesium production efficiency from 71.2 to 73.5% when increasing the second-step calcination temperature from 700 to 800°C, while a notable decrease is observed with further

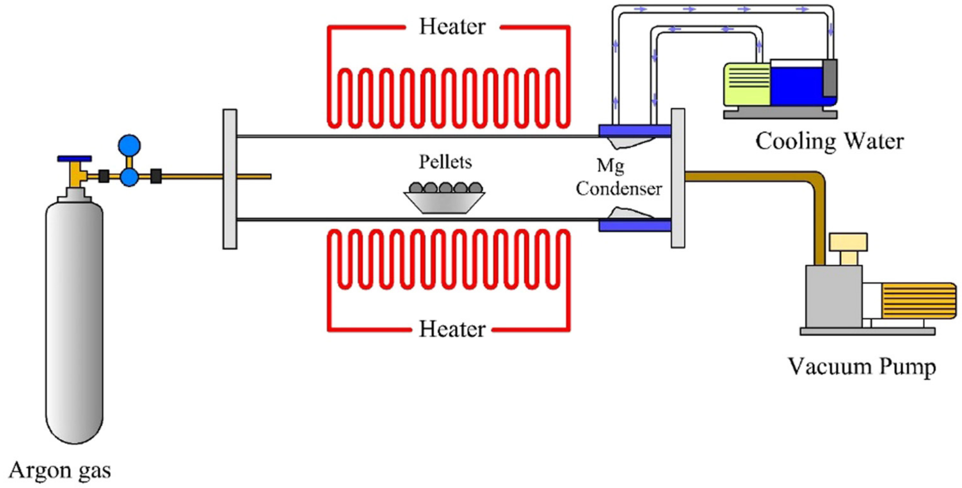

Figure 3: Experimental equipment layout.

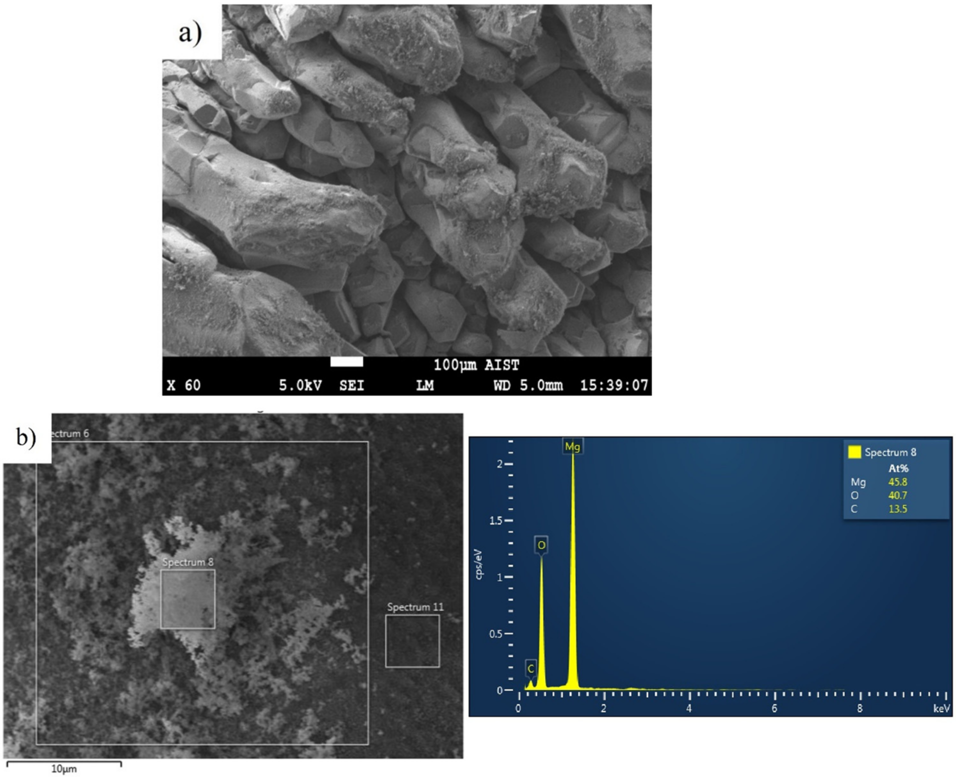

Figure 4: SEM image of the Mg crystal: (a) at the crystallization region and (b) impurities on the Mg crystal surface.

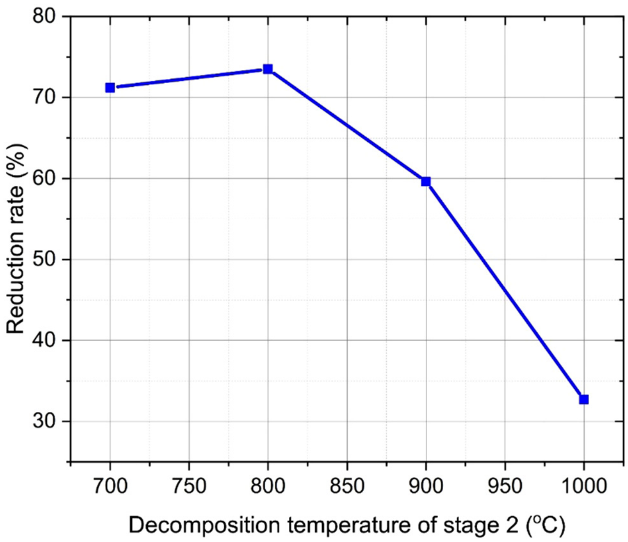

Figure 5: Effect of stage 2 decomposition temperature on reduction efficiency.

increases to 1,000°C. Reduction efficiency at 1,000°C heating is only 32.7%. This decline in efficiency at higher calcination temperatures is attributed to the accelerated carbonate decomposition reaction. At elevated temperatures, the generated CO_2 gas diffuses rapidly through the pellet, causing structural disruption and increased porosity or fragmentation. Consequently, reactant proximity decreases, impeding reaction rates during the reduction phase.

To elucidate this phenomenon, select experiments involved rapid cooling of pellets with Ar gas after a 1-h heating period, allowing observation of pellet morphology. The results depicted in Figure 6 reveal that pellets calcined at 700 and 800°C have the same color and shape as the initial pellets, with minimal alteration in size. Conversely, pellets subjected to 900 and 1,000°C heating exhibit yellow and brown discoloration, accompanied by surface cracks. Particularly at 1,000°C, pellets undergo fragmentation, diminishing the likelihood of reactant contact during the reduction phase.

Figure 7 presents SEM images illustrating the microstructures of the pellets before and after calcination. Prior to calcination, the pellets exhibit a well-connected structure, with ferrosilicon particles in close contact with the surrounding dolomite particles. However, following calcination at 800 and 1,000°C, a significant increase in porosity is observed, particularly in the sample calcined at 1,000°C. This increase in porosity results in reduced contact between the reactants, which may adversely affect the subsequent reduction stage. During this stage, the reducing agent reacts with dolime to produce Mg vapor. Since this

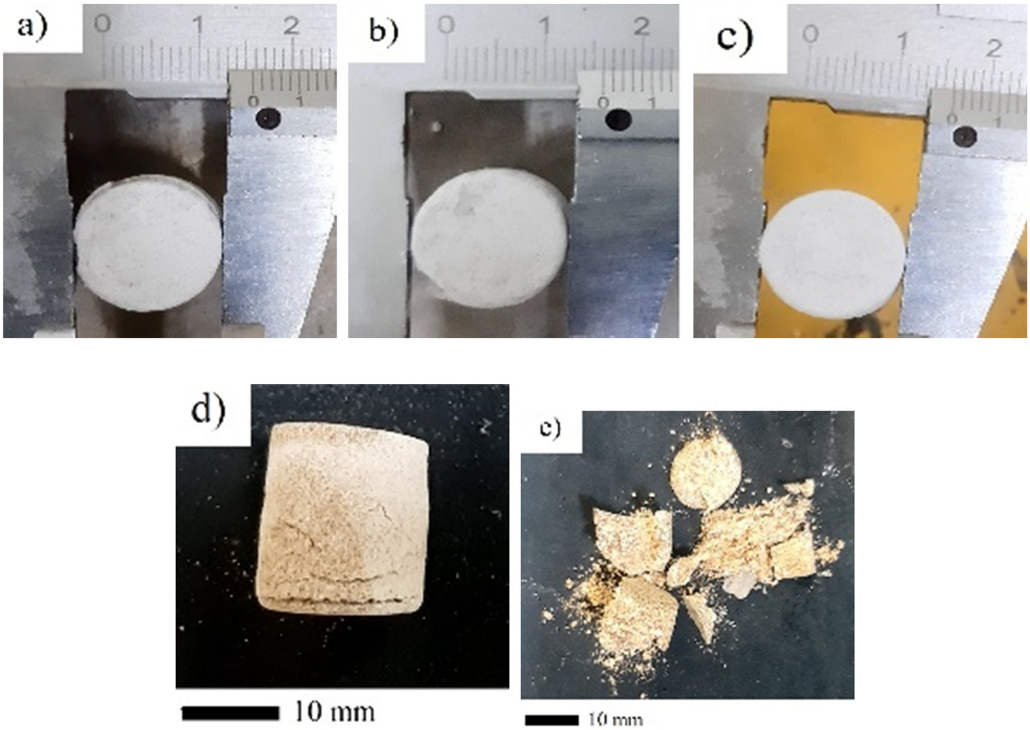

Figure 6: Images of pellets: (a) initial and after decomposition in step 2 at (b) 700°C, (c) 800°C, (d) 900°C, and (e) 1,000°C.

is a solid–solid reaction, maintaining adequate contact between the reactants is essential to facilitate the reduction process. This partially explains the significant decline in reduction efficiency observed when the calcination step is conducted at elevated temperatures.

The XRD analysis results of the decomposed samples are depicted in Figure 8, revealing distinct phases based on the calcination temperatures. Samples subjected to second-step calcination temperatures of 700 and 800°C predominantly exhibit phases consistent with the original mixture composition, including CaO, MgO, and Si. Additionally, the appearance of the $Ca(OH)_2$ phase was observed, which was attributed to the hydration of CaO in ambient humidity. Consequently, the reduction efficiency of these samples is lower compared to the traditional Pidgeon process, as the release of CO_2 gas increases pellet porosity.

Conversely, samples calcined at 900 and 1,000°C exhibit main phases comprising MgO, $CaSi_2$, and Ca_2SiO_4. This indicates substantial CaO reacting with Si to form $CaSi_2$ and Ca_2SiO_4, consequently increasing the residual waste levels in the mixture pre-reduction. Notably, the sample subjected to 1,000°C calcination displays the presence of the Fe_2O_3 phase, accounting for its brown coloration. Weak intensity diffraction peaks of SiC further suggest the occurrence of oxidation reactions between CO_2 and ferrosilicon at 1,000°C in a vacuum of 1,000 Pa, resulting in SiC and Fe_2O_3 product formation. It can be predicted that the oxidation reaction of ferrosilicon with

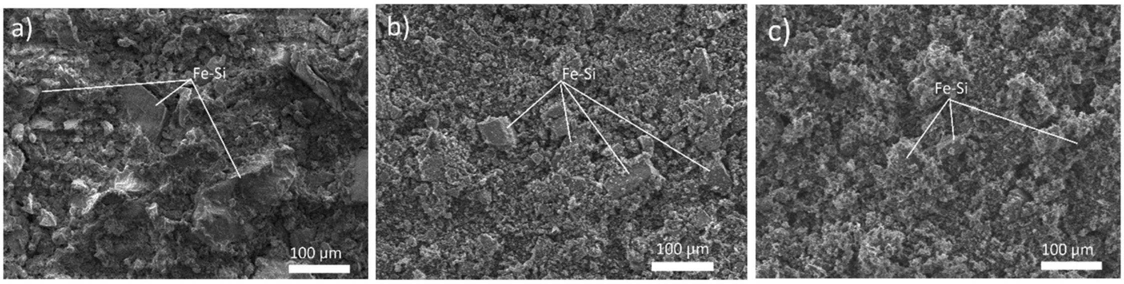

Figure 7: SEM images of pellets (a) before calcination, (b) after calcination at 800°C, and (c) after calcination at 1,000°C.

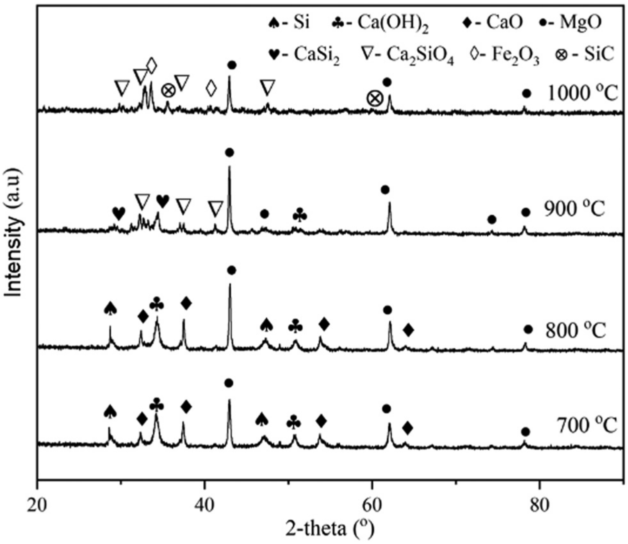

Figure 8: XRD analysis of pellets after calcination at different temperatures.

CO_2 occurring during calcination at 1,000°C affects the efficiency of the reduction stage. Ferrosilicon 75% mainly consists of two phases: Si and $FeSi_2$ [3]. From the formation of phases in the coal pellet after calcination, it is inferred that CO_2 reacts with ferrosilicon according to the following reactions:

$$CO_{2(g)} + 2Si_{(s)} \rightarrow SiC_{(s)} + SiO_{2(s)}, \tag{3}$$

$$CO_{2(g)} + FeSi_{2(s)} \rightarrow Fe + SiC_{(s)} + SiO_{2(s)}, \tag{4}$$

$$CO_{2(g)} + Fe_{(s)} \rightarrow Fe_2O_3 + CO_{(g)}, \tag{5}$$

$$CaO_{(s)} + SiO_{2(s)} \rightarrow Ca_2SiO_{4(s)}. \tag{6}$$

During the calcination stage, CO_2 gas generated from the decomposition of dolomite diffuses through the pores of the coal pellet and reacts with the Si and $FeSi_2$ phases in ferrosilicon, forming Fe, SiC, and SiO_2 according to reactions (3) and (4). The SiO_2 product then readily reacts with CaO to form Ca_2SiO_4 according to reaction (5), and Fe continues to oxidize in the CO_2 environment, forming Fe_2O_3 according to reaction (6). This explains why phases of Fe_2O_3 and Ca_2SiO_4 with high diffraction intensity were observed, while CaO diffraction was almost absent in pellets calcined at 1,000°C. The occurrence of these reactions consumes a significant amount of reducing agent and CaO, which greatly impacts the reduction efficiency in the subsequent stage.

Thus, lower decomposition temperature can reduce the oxidation of ferrosilicon by CO_2 and conserve the amount of reductant for the next reduction stage. Within the decomposition temperature range studied, the optimal decomposition temperature for the second step in this integrated process is determined to be 800°C. This temperature ensures complete dolomite decomposition without inducing reactions between CO_2 and the reducing agent while also preserving the bonding ability between reactants.

3.3 Effect of forming pressure on reduction efficiency

The study on the influence of forming pressure was conducted with samples subjected to a first-step decomposition temperature of 500°C and a second-step temperature of 800°C, with reduction times ranging from 0.5 to 3 h. As shown in Figure 9, the reduction rate changed significantly when the forming pressure increased from 60 to 150 MPa. After 1 h, the reduction efficiency of pellets with a forming pressure of 150 MPa exceeded 60%, while pellets with a pressure of 60 MPa only achieved slightly over 40%. This indicates that the release of CO_2 gas during heating creates voids, reducing the pellet density. Increasing the forming pressure enhances the compressive strength of the pellets and increases the contact area between the reacting particles, leading to a higher reduction rate for pellets with higher pressure.

However, between 1 and 3 h, the reduction rate of the 120 and 150 MPa pellets began to show signs of slowing down. After 3 h, the reduction efficiency for all five samples with varying forming pressures converged, ranging from 73 to 77%. This suggests that while forming pressure influences the rate of the reduction reaction, it does not impact the final reduction efficiency of the overall process.

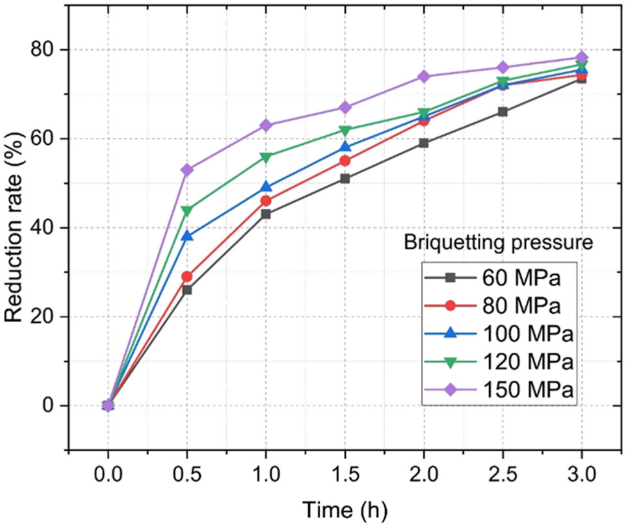

Figure 9: Effect of forming pressure on reduction efficiency.

4 Conclusion

The study assessed the feasibility of the integrated process. On an experimental scale, the integrated method produced satisfactory results, with only a slight decrease in reduction efficiency compared to the traditional Pidgeon method. A key finding was that the calcination temperature during the integrated process had a significant impact on reduction efficiency. The optimal reduction efficiency was achieved with calcination temperatures of 500°C for the first step and 800°C for the second step. While forming pressure greatly influenced the reduction reaction rate, it did not significantly affect the final reduction efficiency.

Acknowledgements: The study was supported by the School of Mechanical Engineering, Vietnam Maritime University.

Funding information: Authors state no funding involved.

Author contributions: All authors have accepted responsibility for the entire content of this manuscript and consented to its submission to the journal, reviewed all the results and approved the final version of the manuscript. VVQ was responsible for project design and experimental data analysis. NDN contributed by designing the experiments and performing them. All authors participated in discussing the results, drafting the manuscript, and providing feedback during the review process.

Conflict of interest: The authors declare no conflicts of interest.

Data availability statement: The data that support the finding of this study are available from the corresponding author upon reasonable request.

References

[1] Zang, J. C. and W. Ding. The pidgeon process in China and its future. In *Essential readings in magnesium technology*, Springer International Publishing, Cham, 2016, pp. 113–116.

[2] Gao, F., Z. Nie, Z. Wang, X. Gong, and T. Zuo. Life cycle assessment of primary magnesium production using the Pidgeon process in China. *International Journal of Life Cycle Assessment*, Vol. 14, No. 5, 2009, pp. 480–489.

[3] Vu, Q. V., T. T. T. Vu, C. M. Doan, B. N. Duong, and H. D. Tran. Silicothermic reduction of thanh hoa dolomite: Thermodynamic and experimental. *Acta Metallurgica Slovaca*, Vol. 27, No. 3, 2021, pp. 109–113.

[4] Gao, F., Z. Nie, Z. Wang, X. Gong, and T. Zuo. Assessing environmental impact of magnesium production using Pidgeon process in China. *Transactions of Nonferrous Metals Society of China*, Vol. 18, No. 3, Jun. 2008, pp. 749–754.

[5] Ramakrishnan, S. and P. Koltun. Global warming impact of the magnesium produced in China using the Pidgeon process. *Resources, Conservation and Recycling*, Vol. 42, No. 1, 2004, pp. 49–64.

[6] Tian, Y., L. Wang, B. Yang, Y. Dai, B. Xu, F. Wang, et al. Comparative evaluation of energy and resource consumption for vacuum carbothermal reduction and Pidgeon process used in magnesium production. *Journal of Magnesium and Alloys*, Vol. 10, No. 3, 2022, pp. 697–706.

[7] Prentice, L. H. and N. Haque. MagSonicTM carbothermal technology compared with the electrolytic and pidgeon processes. S. N. Mathaudhu, W. H. Sillekens, N. R. Neelameggham, N. Hort, (eds), Magnesium Technology, Springer, Cham, 2012, pp. 37–41.

[8] Abdellatif, M. Review of the development work on the Mintek Thermal Magnesium Process (MTMP). *Journal of the Southern African Institute of Mining and Metallurgy*, Vol. 111, No. 6, pp. 393–399. 2011.

[9] Quyen, V. V., V. T. T. Trang, N. D. Nam, T. D. Huy, and D. N. Binh. Research on the manufacturing magnesium from thanhhoa dolomite by pidgeon process. *EUREKA, Physics and Engineering*, Vol. 2020, No. 6, 2020, pp. 97–107.

[10] Fu, D., T. Zhang, Z. Dou, and L. Guan. A new energy-efficient and environmentally friendly process to produce magnesium. *Canadian Metallurgical Quarterly*, Vol. 56, No. 4, 2017, pp. 418–425.

[11] Fu, D. X., T. A. Zhang, L. K. Guan, Z. H. Dou, and M. Wen. Magnesium production by silicothermic reduction of dolime in pre-prepared dolomite pellets. *JOM*, Vol. 68, No. 12, 2016, pp. 3208–3213.

[12] Chen, Y., G. Mai, Y. Che, and J. He. Novel efficient reduction route for magnesium production using silicothermic process. *Materials*, Vol. 15, No. 17, 2022, id. 6009.

[13] Guo, J., T. Zhang, D. Fu, J. Han, Z. Ji, and Z. Dou. Research on properties of prefabricated pellets of silicothermic process after calcination in flowing argon atmosphere. J. Jordon, V. Miller, V. Joshi, N. Neelameggham, (eds), *Magnesium Technology*, Springer, Cham, 2020, pp. 303–308.

[14] Zhang, C., C. Wang, S. Zhang, and L. Guo. The effects of hydration activity of calcined dolomite (HCD) on the silicothermic reduction process. *International Journal of Mineral Processing*, Vol. 142, 2015, pp. 154–160.

[15] Wen, M., T. Zhang, Z. Dou, Y. Guan, and R. Zhang. Two-stage calcination of dolomite pellets for mg-extraction by silicothermic reduction in vacuum. *Zhenkong Kexue yu Jishu Xuebao/Journal of Vacuum Science and Technology*, Vol. 34, No. 11, 2014, pp. 1242–1245.